An automatic reconstruction method of fibula for mandibular defect

Ruiming Huang[1,*], Junlei Hu[2], Jiannan Liu[2]

[1.] School of Electronic Information and Communications, Huazhong University of Science and Technology, Wuhan 430074, China

[2.] Department of Oral Maxillofacial - Head & Neck Oncology, Shanghai Ninth People's Hospital Affiliated to Shanghai Jiao Tong University School of Medicine, Shanghai 200011, China.

Corresponding author: Ruiming Huang

E-mail: huang_rm@qq.com

Abstract. Purpose: For patients who need to reconstruct the mandible with the fibula, this article gives an automated design scheme to save the doctor's time. Methods: First, perform the initial registration by analyzing the characteristic points of the fibula and jaw defect, cut the fibula and move it to the approximate location. Then optimize and adjust, and finally give a plan. Results The average operating time is about 10s for each reconstruction planning. Six surgeons at different levels were invited to rate the output of our method and manual operations by expert and novice, the evaluation of our method is even higher than that of the experts. Conclusions: The proposed method can automatically accomplish the task. At the same time, it is self-defining, allowing doctors to select the required feature points based on their own experience. This design has application value in the design of surgical plan.

Keywords: Mandible Tumor, Mandible reconstruction, Automated surgical planning.

1. Introduction

Mandibular tumor is prone to occur in young people. For malignant tumors, the mandible needs to be amputated and get defected. The recovery of functional appearance after surgery is very important for young patients. [1,2] After the removal of the mandibular tumor, in order to restore the patient's mandibular function and appearance, the current "gold-standard" repair method is the use of free fibula flaps for vascularized autologous bone grafts to repair the defective jaw.[3,4]

After Hidalgo [5] first reported the application of the fibular flap in maxillofacial surgery and plastic surgery, many literatures reported on the anatomy, flap retrieval method and clinical application of the fibular flap. However, the shaping and positioning of the fibula flaps are difficulties in the operation. At present, there are methods to determine the fibula shaping plan based on the characteristics of the jaw. For example, the Chinese team of scientists summarized various common situations of surgery and obtained a series of experience.[6] They classify the mandibular defect, analyze it, and make a comprehensive judgment to give a plan. Most of these cases are based on the experience of doctors, the characteristic points used are not some special points, but the overall structure. Forementioned example also shows that many factors need to be considered in this operation. If the feature points are extracted separately, the recognition accuracy may decrease, without taking the shape of the patient's jaw into full consideration.

Moreover, in the current surgical plan design software, such as ProPlan (Materialise, Belgium)[7], doctors are required to constantly adjust the design and reconstruction plan based on their own experience[8], which is time-consuming and labor-intensive. The workflow of using the long shaft bone to fit non-linear mandibular defect is basically fixed, and some process of determining the initial plan is mechanical. Previous teams have designed a method to automatically generate a complete mandible from a defective mandible based on a training set.[9] However, in actual medical treatment, the method of autologous transplantation is mostly used, and the application scope of the

complete filler is not wide; at the same time, the steps such as labeling in the method require manual operation, which is only a semi-automatic process.

Therefore, this article is dedicated to design an automatic fibula reconstruction algorithm based on the shape of the complete side for cases where one side is still intact. After the computer reads the patient's part model, the shape of the mandible and fibula is considered, and the position, angle, and combination of the fibula segment are automatically adjusted based on computer calculation and analysis. Finally, an optimized plan is given successfully to realize the automatic shaping of the fibula reconstruction, so as to save the time and energy of the initial plan design of the operation. Previous teams have demonstrated through experiments that there are certain differences in the shape of the mandible between human and ethnic groups[10].

2. Method

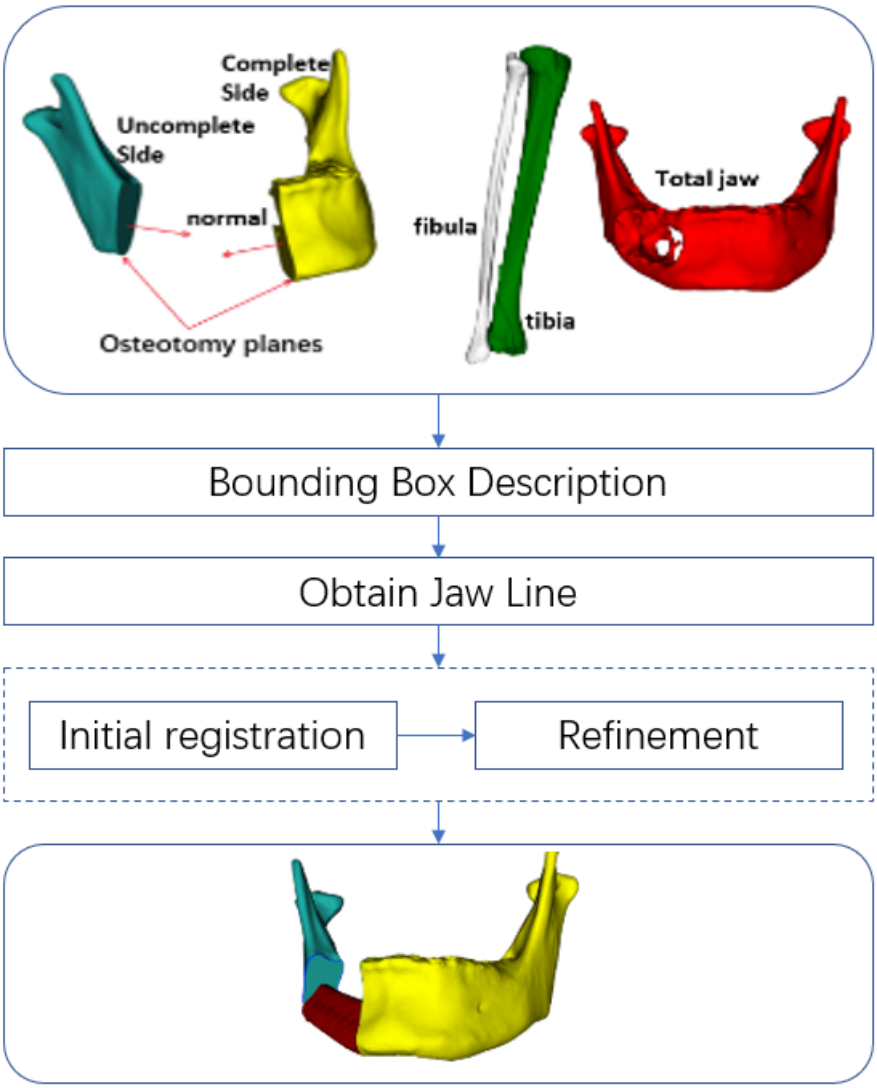

Figure 1. Overall work flow of automatic reconstruction method.

Figure 1 is a description of the entire algorithm workflow. First, input fibula, tibia, unhealthy jaw (include complete side and uncomplete side after surgical resection of the tumor), total jaw models and two osteotomy planes (include their normal and origin). Then describe the position of the mandibular line as well as determine the points for the initial registration. The next step is the initial registration, which is to cut the fibula and move it to the jaw defect. Then optimize and adjust to a more appropriate position. Finally output the result.

2.1 Obtain the jaw line: Bounding-Box-Based description

In order to reach a result of good aesthetic and functional, our important goal is to align fibula with the jaw line as much as possible, which is also an important factor in evaluating the quality of position matching. The jaw line refers to the contour line of the bone at the bottom of the face. Figure 2 shows its part in jaw.

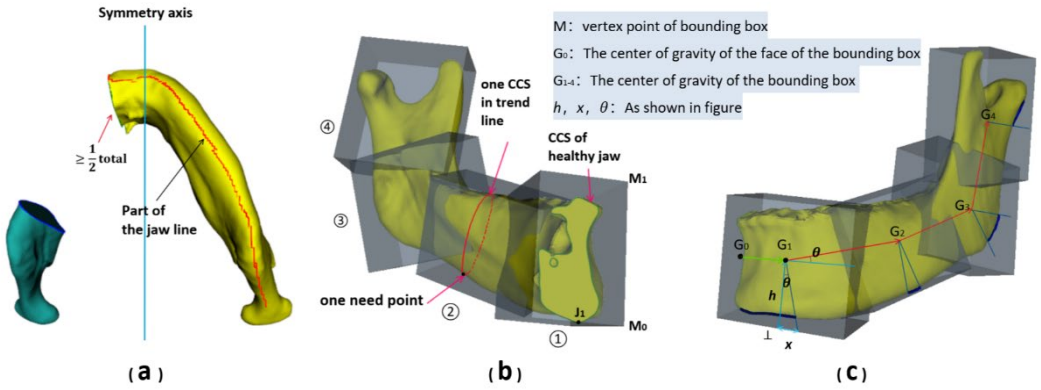

Figure 2. (a) The jaw line's part in complete jaw; (b) OBB-tree for the complete side of the jaw and some information, the green and red curves present the contour of the cross-section (CCS) (c) Trend line and improvement.

The Figure 2(a) is a top view of the jaw line of a complete side jaw. Since the intact side of the jaw is larger than half of the whole, the whole can be found. The defective part is able to be approximated by symmetrical of obtained jaw line.

In order to find the jaw line, we introduce the following concepts. Oriented Bounding Box (OBB) is essentially a cuboid that is closest to the object, but the cuboid can be rotated arbitrarily according to the first moment of the object. Thus, the OBB is used to describe the approximate position and general shape of the model. The OBB tree is a hierarchical tree structure of such boxes, where deeper levels of OBB confine smaller regions of space. [11] The Figure 2(b) is the result of finding the OBB-tree for the complete side of the jaw.

According to the natural shape of mandible, a 2-level OBB-tree can be used to enclose the complete jaws. M0 and M1 are two vertex points of bounding box ①, and line M0M1 can be used to approximate the direction of gravity, as shown in the Figure 2(b).

In order to determine the intersection of the jaw line and each CCS, the tangent point was utilized to approximate the feature point, the purpose is to describe the edge of one object. Here the model is composed of discrete points, so the definition of the tangent point is the point with the shortest distance to a given plane among a series of points on the CCS, and this can be solved by traversal and distance formulas. Calculate this distance for each point on the CCS. If it is smaller than the current minimum value, update the minimum value to this distance. After the traversal is completed, the point corresponding to the minimum value is the desired point.

In this method, we give the required lowest plane as follows. The gravity direction vector and M0 can be used to determine the lowest plane crossing M0. In order to ensure the stability of the zero-potential energy surface and prevent it from intersecting with the model, the symmetrical point of M1 with respect to M0 is finally selected and the plane with the direction of gravity as the normal vector is used as the zero-potential energy surface. Obviously, we only need to find the point closest to the plane on the CCS of the complete jaw, it can be approximated as a jaw line point, called jaw1 point.

Further, find a line to depict the direction of the jaw. Then we can take some points equidistantly on this "trend line", and use each point as the origin, the direction of the trend line here as the normal to determine a plane, and get each CCS with the jaw. For each CCS, find the need point corresponding to the minimum distance from the zero-gravity potential energy surface. As Figure 2(b) shows. The

calculated need point can be approximated as the jaw line when it reaches a certain degree of subdivision. The next step is to find the appropriate "trend line".

The connection of the centroids (G1, G2, G3, G4) of the four bounding boxes can be roughly used as a trend line, as shown in the Figure 2(c). Obviously, line G3G4 can ensure that it is not perpendicular to the bottom surface. That is, there will be no situation where the CCS is parallel to the bottom surface and the closest distance point required cannot be found.

However, the detailed jaw line in the region of start and junction cannot be delineated yet. As Figure 2(c) shows, there is no CCS in the dark blue area. Therefore, this part of the jaw line cannot be obtained. So next we use geometric methods to optimize this part. Line G0G1 is able to supplement one part of the missing line, for the initial start position G0 is not at the beginning of OBB. The dark blue area on the top will be ignored. The second type of improvement is due to the fact that we use line segments instead of smooth lines to approximate the "trend line". It causes that the other dark blue areas not be swept by the cutting plane. After geometric analysis, in each junction, the approximate length of the missing line is

$$X = h\tan\theta \tag{1}$$

The geometric relationship is shown in the Figure 2(c). Such an offset needs to be considered when the direction changes: G0G1 to G1G2, G1G2 to G2G3, G2G3 to G3G4, and a total of three are required. For example, when cutting along G0G1, add X as an offset to the initial traversal length $|01\quad|$. Finally, add the calculated points to a pointset, which can approximate the jaw line.

2.2 Initial registration

In the previous step, we calculated the jaw line and obtained some features that can be used for registration. In order to determine the initial registration from fibula to the defect in mandible, two corresponding pointsets on two parts, $\boldsymbol{P}_A = \{P_A^1, P_A^2, \dots P_A^n\}$,$\boldsymbol{P}_B = \{P_B^1, P_B^2, \dots P_B^n\}$. Let T_B^A be the transformation matrix, the relationship is

$$\begin{bmatrix} P_A^1 \\ P_A^2 \\ \dots \\ P_A^n \end{bmatrix} T_B^A = \begin{bmatrix} P_B^1 \\ P_B^2 \\ \dots \\ P_B^n \end{bmatrix} \tag{2}$$

By the least square method, we can get[12]

$$T_B^A = (P_L P_L^T)^{-1} P_R \tag{3}$$

where $P_L = \begin{bmatrix} P_A^1 \\ P_A^2 \\ \dots \\ P_A^n \end{bmatrix}$, $P_R = \begin{bmatrix} P_B^1 \\ P_B^2 \\ \dots \\ P_B^n \end{bmatrix}$

The above method of obtaining the rotation matrix T_B^A by minimizing the average distance between the target point and the corresponding point of the source point is called the landmark algorithm.

In these cases, we take four sets of points on the fibula and tibia, as shown in the following Figure 3 (for other potentially useful data points, they will be used in the refinement part). Considering that the matching of the jaw line during registration has a greater impact, and the four points in the point concentration are not completely coplanar, when do the landmark, we additionally take some corresponding points on the line J1J2 and line F1F2, which makes the importance of the jaw line strengthened.

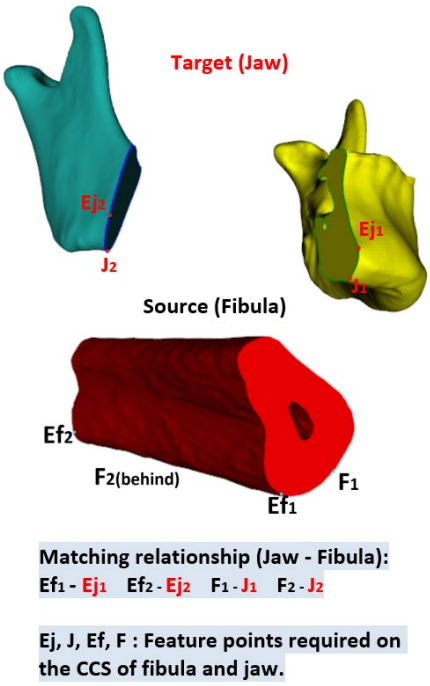

Figure 3. Feature points required by the above algorithm: target and source. ("Edge" "Jaw" "Fibula" is abbreviated as "E" "J" "F")

To find the corresponding point Jaw2, first, find the result of CCS symmetry on the incomplete side of the jaw with respect to the symmetry plane of the jaw, and then use the existing mandibular line to find the required point for this result. The calculation of the symmetry plane can be determined with the help of the bounding box of the total jaw. The calculate process is the same as J1. We will not go into details here, and focus on the method of solving the symmetry point.

Assume that the plane is defined by normal (a, b, c) and origin (x_0, y_0, z_0). For any point X (x_i, y_i, z_i), its projection point on the plane is denoted as $X'(x, y, z)$, the expression of a given plane can be transformed into the following form:

$$Ax + By + Cz + D = 0 \tag{4}$$

where A,B,C,D are the parameters in the plane function.

The straight line XX' is parallel to the normal vector of the plane, so the parameter equation of the straight line is:

$$\begin{aligned} x &= x_i - A * t \\ y &= y_i - B * t \\ z &= z_i - C * t \end{aligned} \tag{5}$$

where t is parameter to be solved.

Put the coordinates of the point (x, y, z) into the plane equation, and you can find the parameter t

$$t = \frac{Ax_i + By_i + Cz_i + D}{A^2 + B^2 + C^2} \tag{6}$$

Then put t into the parametric equation of the straight line to find the projection point $X'(x, y, z)$, use the midpoint coordinate formula to get the coordinate of the point J2.

In this way, the distance between Jaw1 and Jaw2 can be used as the approximate length to intercept the fibula. Taking into account that the jaw section is not necessarily completely vertical, and the actual surgery may need it to be longer to ensure the fault tolerance in actual use, a slightly longer fibula can be truncated within a reasonable range (the length is not more than 1.1 times the above distance), and the fibula is surrounded by an OBB. By analyzing the data points (vertices) of the fibula bounding box, the vector direction corresponding to the longest side vector and the side length

of the remaining two bounding boxes can be obtained. Then you can use the direction of the fibula as the normal vector direction of the tangent plane, take the quarter position as the starting point, and use the bounding box origin N0 to perform vector operations along the fibula direction to express the desired point on the section.

By finding the longest side, we can get the information of "fibula direction", which is represented by the vector where the longest side is located. As shown below in Figure 4.

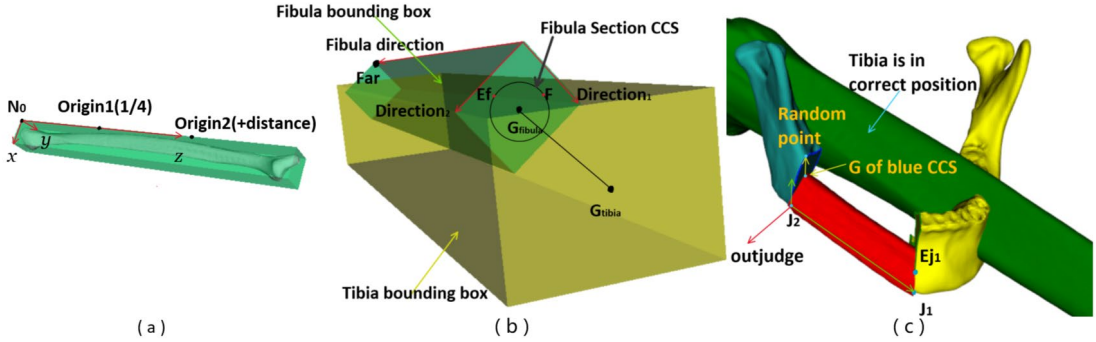

Figure 4 (a). The OBB of fibula and analyze. (b) Use a circle to represent the CCS of the fibula section. the bounding box of the fibula (top left, green) and tibia (bottom right, yellow). (c)The initial registration result and some details.

The existence of blood vessels needs to be considered in the next step. First consider the point F1 corresponding to J1. Since the fibular vessels cannot be on the outside, when selecting these points, be care to make the resulting fibular vessels on the inside (close to the teeth).

As shown in the Figure 4(b), since the fibula blood vessels are on the same side of the tibia, the tibia model is used to infer the blood vessel position. To determine the position of the tibia, the line connecting the centroids of the two OBB is approximately perpendicular or parallel to the two vectors (direction1,2) on the fibula bounding box obtained before excluding the long side normal vector, which can facilitate us to find the required normal vector. Then just get the points to determine the plane. Finding the farthest vertex from Gtibia “far” among the eight vertices of the fibula bounding box can help us achieve the following effects:

In Figure 4(b), the centroid of the tibia bounding box is (Gtibia). The farthest point from Gtibia in the vertex of fibula bounding box is Far. Find the two sections of the fibula and the CCS of the fibula respectively, and tangent (find the nearest point) to the two sections at Fibula (F) and Edge of fibula (Ef). The reason for using the two sets of points instead of the opposite side of Fibula is because the shape of the fibula is small at the top, big at the bottom. The jaw model is the same, thus the corresponding shape is more appropriate.

Correspondingly, in order to make the alignment match accurately, find a point Edge of jaw (Ej) outside the CCS of each group of Jaw points and make the distance from J to Ej equal to the distance from each F to Ef. That is $|JEj| = |FEf|$.

As shown in the Figure 4(c).

$$\overrightarrow{\text{outjudge}} = \overrightarrow{J_2J_1} \times \overrightarrow{(-\text{gravity})} \tag{7}$$

If $\overrightarrow{outjudge} \cdot \overrightarrow{GRandomPoint} \geq 0$, $RandomPoint$ is in the outside of the CCS.

For the principle, considering the spatial relationship of the position, the uncertain factors of rotation also need to be considered. As shown in Figure 4(c), if the complete side and uncomplete side are exchanged positions, because the interception of the key points in the fibula is uniquely determined by the tibia, it is equivalent to that the fibula needs to be rotated 180 degrees horizontally to match the corresponding CCS. When point matching, this will inevitably cause the Ef to turn to the inside. By comparing the number of model data points, we can determine which side is the complete jaw. For situations that need to be corrected, when obtaining the Ej of the uncomplete jaw CCS, pay attention to swapping the distance between the two sets of F and the Ef point on the fibula CCS. When performing landmark, swap Jaw1,2 and Ej1,2 of the target point set respectively.

2.3 Refinement

After the initial registration, the purpose of the refinement is improving the smoothness and continuity in the connection parts of fibula and mandible.

We take a series of corresponding data points on the outside of the jaw and fibula CCS, depict the trend of each place, and design a method to quantitatively compare the difference between the two trends at this time. At runtime, an optimal solution can be evaluated by adjusting the rotation angle of the fibula within a suitable range. Among them, it is obvious that the CCS and Jaw, Ej data of the jaw are fixed, and the remaining data need to be updated in real time to ensure the alignment of the jaw line.

First determine the axis of rotation. As shown in Figure 5(a), the connection two G of the fibula CCS is the rotation axis, and set the rotation traversal range. Then enter the automatic update module, for each rotation, use the previous zero potential energy surface to find a new fibula CCS and its tangent point, which is recorded as Fibula_ro1,2. Because the jaw is fixed, the distance between Jaw and Ej in the previous initial registration can be used to obtain a new Edge of Fibula_ro1,2 each time according to the previous method of finding Ej. Then use these as source points now: Fibula after rotation1,2 (F after rotation) and Edge of Fibula after rotation1,2 (Ef after rotation) to find the landmark at this time. Perform landmark transformation on the rotated CCS to get the new matching position.

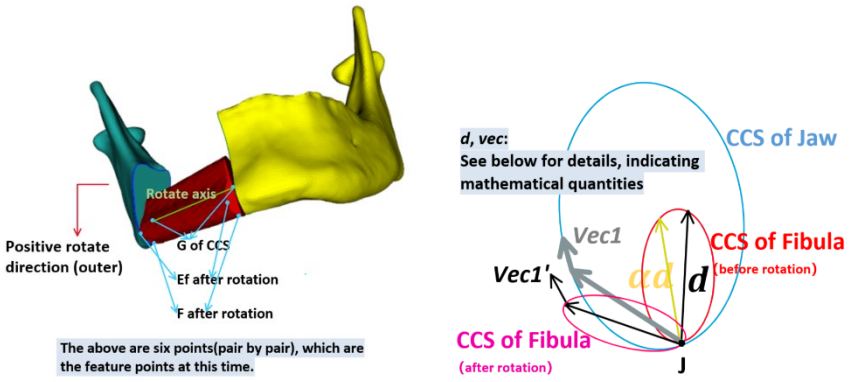

(a) (b)

Figure 5. (a) Rotation details. (b) Diagram of the evaluation algorithm.

The next step is to evaluate the module. For the CCS of the fibula and the jaw, the Jaw point is taken as the starting point, and the farthest distance from J to the outer CCS at the time of initial registration is recorded as d. Analogous to the design idea of Edge, we look for some equidistant data points from the beginning of Jaw to the end of CCS on the fibula model and the jaw model as sampling points. As shown in Figure 5(b), an ellipse is used to approximate the CCS, where the value range of α is between 0-1, which indicates the degree of subdivision. Taking into account the efficiency and the shape and trend of the curved surface at CCS is relatively simple, we use 0.1 as the scale, and find $0.1d, 0.2d \ldots d$.

Since these two CCSs are almost coplanar, we can convert from three dimensions to two dimensions, simplify the calculations with the idea of "dimensionality reduction", and analyze the trend differences of corresponding points in the two dimensions. Based on the idea of derivative, the "point vector" formed by each point and its nearest CCS data point is close to the tangent of the curve here, describing the general trend of this point. Thus, for each set of corresponding points, find the cos value of the angle between the two vectors, and sum the angles between the jaws and fibula on both sides of a total of 20 sets of vectors. The larger the sum, the larger the cos value, that is, the closer the two trends are.

$$\text{sum} = \sum_{i=1}^{20} \frac{|\overrightarrow{vec_1} \cdot \overrightarrow{vec_1'}|}{|\overrightarrow{vec_1}||\overrightarrow{vec_1'}|} \tag{8}$$

In Figure 5(b), vec1 and vec1' are used to represent a set of "point vectors" of corresponding points. Among them, vec1' represents a point's direction vector on the fibula after rotation, and vec1 represents the corresponding point's direction vector on the jaw. By evaluating the results of the above rotation, the optimal solution under this algorithm can be found.

3. Result

In this section, we designed quantitative and qualitative experiments for evaluating the output of our method.

3.1 Experimental Setup

The method was developed mainly based on opensource library, Visualization Tool Kit (VTK), in Python 3.9 environment. The 3D craniofacial and angiographic models are from Shanghai Ninth People's Hospital.

3.2 Parameter Settings and Evaluation of Speed

In our automatic reconstruction algorithm, there is a tradeoff between accuracy and speed performance. Therefore, we set the division value when solving the trend line at 0.1mm. The interception length is set to 1.1 times the jaw distance. The rotation range during refinement is from -5° to 20° with the iterative step at 1° .

We tested more than 15 sets of data in total, and each set of data was tested multiple times. When the mean length of edges in triangular meshes of mandible and fibular equals 0.55mm, the average running time is 10s.

3.3 Evaluation of Robust

We conduct tests in different situations to ensure robustness. The result shows both sides connection view and pitch view. We tested different defect locations, defect sizes, and complete mandible sizes. There are seven sets of data, corresponding to the following seven cases.

Among them, case 1, 2, 3 are cases where the complete jaw is on the left side of the human body and the length of the uncomplete jaw changes. Case 6, 7 is the opposite of the above. Especially, in case 4 and 5, the length of the complete jaw is less than one-half, indicating that the algorithm is universal to a certain extent. The following is the result table. Here we comment on the first case, and the same applies later.

Case 1: Defect of right mandible.

The complete mandible is larger than half of the complete mandible. Defect size: large.

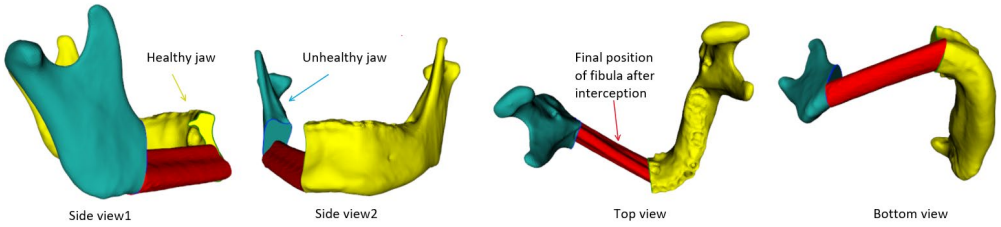

Case 2: Defect of right mandible.

The complete mandible is larger than half of the complete mandible. Defect size: middle.

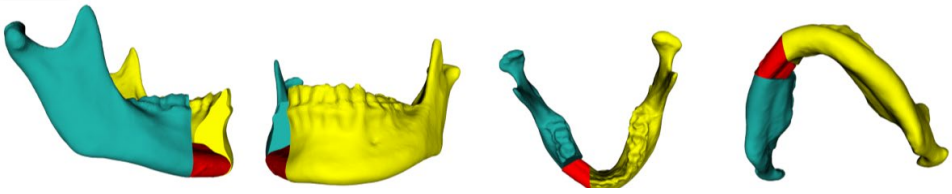

Case 3: Defect of right mandible.

The complete mandible is larger than half of the complete mandible. Defect size: small.

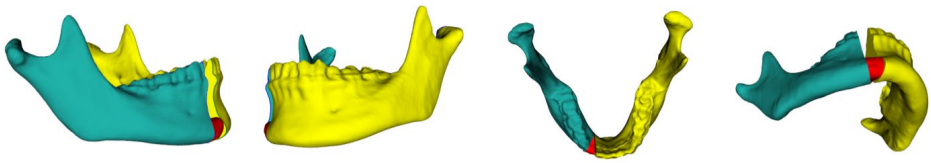

Case 4: Defect of right mandible.

The complete mandible is a little small than half of the complete mandible. Defect size: larger.

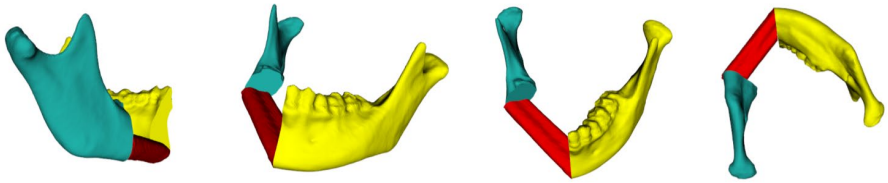

Case 5: Defect of right mandible.

The complete mandible is a little small than half of the complete mandible. Defect size: largest.

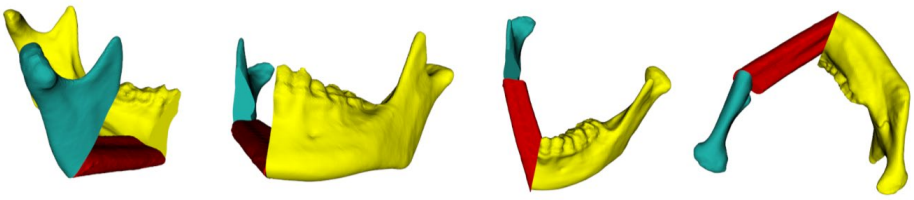

Case 6: Defect of left mandible.

The complete mandible is larger than half of the complete mandible. Defect size: small.

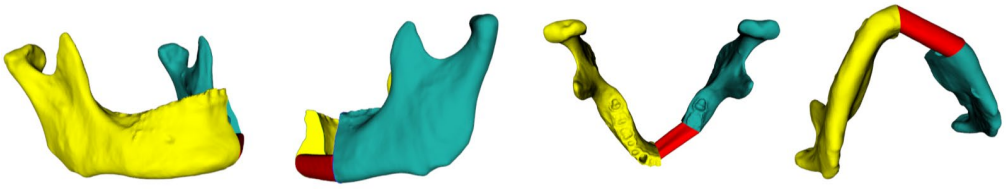

Case 7: Defect of left mandible.

The complete mandible is larger than half of the complete mandible. Defect size: smallest.

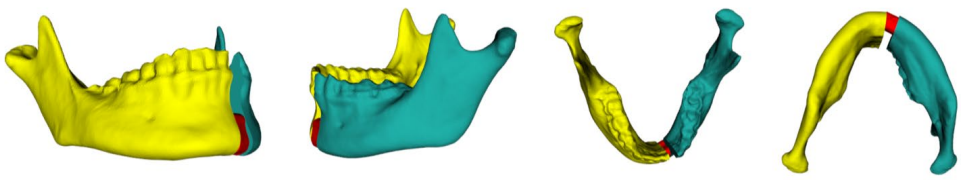

Figure 6. Experimental results. As shown above: Yellow indicates complete jaws. Blue represents uncomplete jaws. Red represents the final position of the fibula after interception. Each row represents a result. The four figures from left to right represent the side view, the top view, and the bottom view.

3.4 Qualitative Evaluation of Output

In order to validate the final performance of the automatic reconstruction method, six surgeons at different levels were invited to rate the output of our method and manual operations by expert and novice. Table 1 shows the qualitative results.

Table 1. The qualitative results of our method.

	Rater 1	Rater 2	Rater 3	Rater 4	Rater 5	Rater 6
Our Method	++	+++	+++	++	++	+++
Expert	+++	++	+++	++	++	++
Novice	+	+	++	+	++	+

Legend: +++: Very Good; ++: Good; +: Not So Good

In this table, our method is highly appreciated by all of the raters. They compared the results of our method with the experts' and the novices', and it undoubtedly comes that our method is better than a novice. Half of the raters said that our method was as accurate as an expert. The other 2 raters even gave our method a better evaluation than the experts'. In a word, all surgeons gave good and very good ratings, it comes to a conclusion that our method is great success.

4. Discussion and conclusion

In the initial registration, we select four sets of points. It is almost impossible to match the fibula and the jaw perfectly, if the landmark algorithm introduces more "edges", the different shapes of the fibula and the jaw will cause a greater degree of non-coplanarity, which will cause uncontrollable confusion.

When solving the trend line, we optimized the final result by finding the offset. But the offset is the value estimated by the geometric method after all, and it needs to be adjusted in actual use. After experiments, the offset is slightly larger. Although it does not affect the description of the jaw line (because the jaw line itself is a series of points, it will only cause the points in a certain area to be denser, and will not affect other parts). For the three offsets in the text, we will make adjustments when using them. After a rough experiment, for the latter two offsets, the result is slightly 3/2 times the minimum length required. In order to improve efficiency, we reduce the offset by a corresponding multiple in actual use. Of course, this is only an approximate value. For specific situations, the required mandibular line can be further optimized.

In the text, we give a method to solve the mandibular line. This method requires subdividing the trend line and selecting points equidistantly to make the section. Increasing the degree of subdivision within a reasonable range can make the algorithm more accurate, but it will also increase the running time. Due to the high precision of the model file in this experiment, considering the accuracy and running time at the same time, we set the distance to 0.1mm. This value can be adjusted according to the model resolution during application.

A slightly longer interception length is more realistic. During the interception, the starting position of the fibula is selected as a quarter of the position. The interception length is set to 1.1 times the jaw distance in the text. A slightly longer interception length can bring more convenience and fault tolerance to the actual operation, especially when the defect is small, this multiple can be further increased. Finally, keep the part between the two jaw cutting surfaces.

Rotation range and step should be considered. As shown in Figure 5, the outward rotation is specified as the positive direction. Since the blood vessel is directly behind the fibula during the initial registration, too much inward rotation will cause the blood vessel to move below the fibula, and too much outward rotation will cause the blood vessel to move above the fibula, which is unrealistic. The range of outward rotation is relatively larger, but inward rotation will cause the blood vessel to approach the position of the mandibular line, so the range is smaller than that of outward rotation. In the end, the rotation interval selected in this experiment is -5° to 20°. The smaller the step size, the more accurate the result, but considering the efficiency, this experiment selects it as 1°.

Although we got good results in the end, there is room for obvious improvement in many places. For example, the use of bounding boxes to approximate the mandibular line is a rough approximation method for simplicity, convenience and efficiency, which also leads to the fact that the algorithm cannot be very accurate. In this algorithm, we let the computer describe a specific location, and it is natural to think of artificial intelligence ideas, and machine learning can be carried out. In the future, artificial intelligence technology will be adopted to optimize the algorithm.

All in all, the proposed method can accomplish the task and can save the doctor's time. At the same time, it is self-defining, allowing doctors to select the required feature points based on their own experience. Our method has very good results, which can be used as a new function of surgical software such as ProPlan. When doctors use software to simulate surgery, our algorithm directly generates a basic plan for the doctor as a reference. This design has application value in the surgical plan.

References

[1] Hyun H K , Hong S D , Kim J W . Recurrent keratocystic odontogenic tumor in the mandible: A case report and literature review[J]. Oral Surgery, Oral Medicine, Oral Pathology, Oral Radiology and Endodontology, 2009, 108(2):e7-e10.

[2] Ferreira J J, Zagalo C M, Oliveira M L, et al. Mandible reconstruction: history, state of the art and persistent problems[J]. Prosthetics and orthotics international, 2015, 39(3): 182-189.

[3] Hidalgo D A. Fibula free flap: a new method of mandible reconstruction[J]. Plastic and reconstructive surgery, 1989, 84(1): 71-79.

[4] Disa J J, Cordeiro P G. Mandible reconstruction with microvascular surgery[C]//Seminars in surgical oncology. New York: John Wiley & Sons, Inc., 2000, 19(3): 226-234. Hidalgo D A . A new method of mandible reconstruction[J]. Plastic & Reconstructive Surgery, 1989, 84.

[5] Xingzhou Q, Chenping Z, Laiping Z, et al. Deep circumflex iliac artery flap combined with a costochondral graft for mandibular reconstruction[J]. British Journal of Oral and Maxillofacial Surgery, 2011, 49(8): 597-601.

[6] https://www.materialise.com/en/medical/software/proplan-cmf

[7] Essig H, Rana M, Kokemueller H, et al. Pre-operative planning for mandibular reconstruction-a full digital planning workflow resulting in a patient specific reconstruction[J]. Head & neck oncology, 2011, 3(1): 1-7.

[8] Raith S , Wolff S , Steiner T , et al. Planning of mandibular reconstructions based on statistical shape models[J]. International Journal of Computer Assisted Radiology & Surgery, 2016, 12(1).

[9] [Metzger M C , Vogel M , Hohlweg-Majert B , et al. Anatomical shape analysis of the mandible in Caucasian and Chinese for the production of preformed mandible reconstruction plates[J]. Journal of cranio-maxillo-facial surgery: official publication of the European Association for Cranio-Maxillo-Facial Surgery, 2011, 39(6):393-400.

[10] Fang Z , Jiang J , Xu J , et al. Efficient collision detection using bounding volume hierarchies of OBB-AABBs and its application. IEEE, 2010.

[11] Fitzpatrick J M, West J B, Maurer C R. Predicting error in rigid-body point-based registration[J]. IEEE transactions on medical imaging, 1998, 17(5): 694-702.